

**Ice formation on lake surface in winter causes warm season bias of lacustrine
brGDGT temperature estimates**

Jiantao Cao ^{1,2}, Zhiguo Rao ^{3,*}, Fuxi Shi ⁴, Guodong Jia ^{1,*}

¹ State Key Laboratory of Marine Geology, Tongji University, Shanghai 200092, China

² Key Laboratory of Western China's Environmental Systems, Ministry of Education, College of Earth
and Environmental Sciences, Lanzhou University, Lanzhou, 730000, China

³ College of Resources and Environmental Sciences, Hunan Normal University, Changsha, 410081,
China

⁴ Jiangxi Provincial Key Laboratory of Silviculture, College of Forestry, Jiangxi Agricultural
University, Nanchang, 330045, China

**Corresponding authors: Zhiguo Rao (raozhg@hunnu.edu.cn); Guodong Jia (jiagd@tongji.edu.cn).*

15 **Abstract**

16 It has been frequently found that lacustrine brGDGT-derived temperatures are warm season biased
17 relative to measured mean annual air temperature (AT) in the mid to high latitudes, the mechanism of
18 which, however, is not very clear. Here, we investigated the brGDGTs from catchment soils,
19 suspended particulate matter (SPM) and surface sediments in different water depths in the Gonghai
20 Lake in north China to explore this question. Our results showed that the brGDGT distribution in
21 sediments resembled that in the SPM but differed from the surrounding soils, suggesting a substantial
22 aquatic origin of the brGDGTs in the lake. Moreover, the increase of brGDGT content and decrease of
23 methylation index with water depth in sediments suggested more contribution of aquatic brGDGTs
24 produced from deep/bottom waters. Therefore, established lake-specific calibrations were applied to
25 estimate local mean annual AT. As usual, the estimates were significantly higher than the measured
26 mean annual AT. However, they were similar to, and thus actually reflected, the mean annual lake
27 water temperature (LWT). Interestingly, the mean annual LWT is close to the measured mean warm
28 season AT, hence suggesting that the apparent warm season bias of lacustrine brGDGT-derived
29 temperatures could be caused by the discrepancy between AT and LWT. In our study region, ice forms
30 at the lake surface during winter, leading to isolation of the underlying lake water from air and hence
31 higher LWT than AT, while LWT basically follows AT during warm seasons when ice disappears.
32 Therefore, we think what lacustrine brGDGTs actually reflected is the mean annual LWT, which is

33 higher than the mean annual AT in our study location. Since the decoupling between LWT and AT in
34 winter due to ice formation is a universal physical phenomenon in the mid to high latitudes, we
35 propose this phenomenon could be also the reason for the widely observed warm season bias of
36 brGDGT-derived temperatures in other seasonally surface ice-forming lakes, especially the shallow
37 lakes.

38 **Keywords:** lake sediments, aquatic brGDGTs, temperature proxy, seasonality, ice formation

39

40 **1 Introduction**

41 The branched glycerol dialkyl glycerol tetraethers (brGDGTs), including 0–2 cyclopentyl
42 moieties (a–c) and four to six methyl groups (I–III) (Weijers et al., 2007a), are components of the cell
43 membranes of microorganisms ubiquitously found in marine and continental environments and
44 sensitive to ambient environmental conditions (Sinninghe Damsté et al., 2000; Weijers et al., 2006a;
45 Schouten et al., 2013). The relative amounts of methyl groups and cyclopentyl moieties, expressed as
46 methylation index and cyclization ratio of brGDGTs (such as MBT/CBT or MBT'/CBT) in soil
47 brGDGTs, has been proposed to reflect mean annual air temperature (AT) (Weijers et al., 2007a;
48 Peterse et al., 2012). With improved analytical methods, a series of 6-methyl brGDGTs, previously
49 co-eluted with 5-methyl brGDGTs, were identified (De Jonge et al., 2013), which may introduce
50 scatter in the original MBT'/CBT calibration for the mean annual AT (De Jonge et al., 2014). Thus,

51 exclusion of the 6-methyl brGDGTs from the MBT', i.e. the newly defined MBT'_{5ME}, results in
52 improved calibrations (De Jonge et al., 2014; Wang et al., 2016; Wang et al., 2019). Calibrations using
53 globally distributed surface soils for the MBT/CBT, MBT'/CBT or MBT'_{5ME} indices (Weijers et al.,
54 2007a; Peterse et al., 2012; De Jonge et al., 2014) have been widely used for continental AT
55 reconstruction (e.g., Weijers et al., 2007b; Niemann et al., 2012; Lu et al., 2019).

56 BrGDGTs in lake environments were initially thought to be derived from soil input (Hopmans et
57 al., 2004; Blaga et al., 2009), allowing the mean annual AT to be reconstructed from lake sediments.
58 However, when the soil-based calibrations are applied to the lake materials, the estimated
59 temperatures are usually significantly lower than actual local AT (Tierney and Russell, 2009; Tierney
60 et al., 2010; Blaga et al., 2010; Loomis et al., 2011, 2012; Pearson et al., 2011; Sun et al., 2011;
61 Russell et al., 2018), suggesting an intricate brGDGTs response to ambient temperature in aquatic
62 environments. Later, more and more studies reveal that brGDGTs could be produced in situ in lake
63 environments and differ significantly from soil derived brGDGT distributions (Wang et al., 2012;
64 Loomis et al., 2014; Naeher et al., 2014; Hu et al., 2015; Cao et al., 2017) and stable carbon isotope
65 composition (Weber et al., 2015, 2018). The findings of intact polar lipid of brGDGTs, indicative of
66 fresh microbial products, in lake water suspended particulate matter (SPM) and surface sediments
67 (Tierney et al., 2012; Schoon et al., 2013; Buckles et al., 2014a; Qian et al., 2019) further confirm the
68 in-situ production of brGDGTs. Nevertheless, the brGDGT distribution in lake surface sediments has

69 been found to be still strongly correlated with AT. Subsequently, quantitative lacustrine-specific
70 calibrations for AT have been established at regional and global scales (Tierney et al., 2010; Pearson
71 et al., 2011; Sun et al., 2011; Loomis et al., 2012; Shanahan et al., 2013; Foster et al., 2016; Dang et
72 al., 2018; Russell et al., 2018), which have been widely used for AT reconstruction. These
73 lacustrine-specific calibrations may reflect mean annual AT well in low-latitude regions (Tierney et al.,
74 2010; Loomis et al., 2012), such as in the Lake Huguangyan (21°09' N, 110°17' E) in south China (Hu
75 et al., 2015), Lake Donghu (30°54' N, 114°41' E) in central China (Qian et al., 2019) and Lake Towuli
76 (2.5° S, 121° E) on the island of Sulawesi (Tierney and Russell, 2009). However, they usually yield
77 estimates biased to the warm/summer seasons in mid- and high-latitude regions (Shanahan et al., 2013;
78 Foster et al., 2016; Dang et al., 2018), such as in Lake Qinghai (36°54' N, 100°01' E) in the
79 northeastern Tibetan Plateau (Wang et al., 2012), in Lower King pond (44°25' N, 72°26' W) in
80 temperate northern Vermont, U.S.A. (Loomis et al., 2014), and in the Arctic lakes (Peterse et al.,
81 2014). The warm biased temperature estimates in the mid- and high-latitude lakes have been
82 postulated to be caused by the higher brGDGT production during warm seasons (e.g., Pearson et al.,
83 2011; Shanahan et al., 2013).

84 BrGDGT-producing bacteria in soils could be metabolically active, hence producing abundant
85 brGDGTs in warm and humid season, but suppressed in cold and/or dry environments (Deng et al.,
86 2016; De Jonge et al., 2014; Naafs et al., 2017). However, it is presently unclear whether the

87 brGDGTs in lacustrine sediments are mainly produced during the warm season. Investigations on lake
88 water SPM reveal higher concentration of brGDGTs in the water column may occur in different
89 seasons, e.g., in winter in Lake Lucerne in central Switzerland (Blaga et al., 2011), Lake Challa in
90 tropical Africa (Buckles et al., 2014a) and Lake Huguangyan in subtropical southern China (Hu et al.,
91 2016), in spring and autumn in Lower King Pond in temperate northern Vermont, U.S.A. (Loomis et
92 al., 2014), and in warm season in Lake Donghu in central China (Qian et al., 2019). Moreover, the
93 contribution of the aquatic brGDGTs to the sediments is quantitatively unknown, and likely minor
94 considering that brGDGT producers favor anoxic conditions (Weijers et al., 2006b; Weber et al., 2018)
95 that usually prevail in bottom water and sediments, which may discount the application of
96 SPM-derived findings to the sedimentary brGDGTs.

97 In fact, brGDGT-based temperature indices should directly record lake water temperature (LWT),
98 rather than AT, if the brGDGTs in lake sediments solely or mainly sourced from the lake environments
99 (Tierney et al., 2010; Loomis et al., 2014). So, the mean annual AT estimate based on lake
100 sedimentary brGDGTs is valid only when LWT is tightly coupled with AT. However, the relationship
101 between LWT and AT is potentially complex in cold regions, as well as in deep lakes, and the
102 coupling between the two is not always the case, which would hamper the application of brGDGTs for
103 temperature estimates (Pearson et al., 2011; Loomis et al., 2014; Weber et al., 2018). In deep lakes,
104 bottom water temperature usually decouples with AT, together with the predominant production of

brGDGTs in deep water and sediments, causing weak correlations between brGDGT-derived temperature and AT (Weber et al., 2018). For shallow lakes, LWT does not always follow AT either, specifically in winter when AT is below freezing, in cold regions, as has been shown in the Lower King pond (Loomis et al., 2014). However, the decoupling between LWT and AT has not been recognized as a key mechanism for the warm bias of brGDGT-derived temperatures observed widely in the mid- and high-latitude lakes, and seasonal production or deposition of brGDGTs is usually invoked as a cause (e.g., Pearson et al., 2011; Shanahan et al., 2013; Loomis et al., 2014). Here, we hypothesized that the decoupling between LWT and AT in mid- and high-latitude shallow lakes, rather than the warm season production, could have caused the frequently observed warmer temperature estimates from the lacustrine brGDGTs. To test this hypothesis, we investigated the Gonghai Lake (a shallow alpine lake) in north China by collecting SPM and surface sediments in different depths in the lake and soils in its catchment in a hot summer and a cold winter. We analyzed brGDGT distributions in these materials to determine the sources of brGDGTs in the lake and further discussed the possible reasons for the seasonality of brGDGT-estimated temperatures.

2 Materials and methods

2.1 Gonghai Lake

The Gonghai Lake [38°54' N, 112°14' E, ca. 1860 m above sea level (a.s.l.); Fig. 1a and 1b] is

located on a planation surface of the watershed between the Sang-kan River and the Fenhe River at the northeast margin of the Chinese Loess Plateau. The location is close to the northern boundary of the modern East Asian summer monsoon (EASM, Chen et al., 2008; Fig. 1a). The modern local climate is controlled mainly by the East Asian monsoon system, with a relatively warm and humid summer resulting from the prevailing EASM from the southeast, and a relatively cold and arid winter under the prevailing East Asian winter monsoon (EAWM) from the northwest (Chen et al., 2013, 2015; Rao et al., 2016). The mean annual precipitation is ca. 482 mm, concentrated (75%) between July and September (Chen et al., 2013). Its total surface area is ca. 0.36 km² and the maximum water depth is ca. 10 m. Based on a nearby weather station, the measured mean annual AT is 4.3 °C for the past 30 years. The warm season lasts from May to September (Fig. 1c), when column stratification develops with an upper-bottom temperature difference >1 °C. During the winter from November to March, ice forms on the lake surface, and LWT under ice vertically constant at ca. 4 °C, which is significantly higher than AT that is much below the freezing point (Fig. 1c). From April to October, the ice disappears and LWT follows AT closely, demonstrating a coupling between them (Fig. 1c). The vegetation type of the planation surface belongs to transitional forest-steppe, dominated by *Larix principis-rupprechtii*, *Pinus tabulaeformis* and *Populus davidiana* forest, *Hippophae rhamnoides* scrub, *Bothriochloa ischaemum* grassland and *Carex spp.* (Chen et al., 2013; Shen et al., 2018).

2.2 Sampling

In September 2017, five surface soil samples in the catchment and five surface sediment samples at different depths (1.0, 2.5, 5.5, 6.7, 8.0 m) in Gonghai Lake were collected (Fig. 1b). At each soil sample site, we collected 5–6 subsamples (top 0–2 cm) within an area of ca. 100 m² with contrasting micro-topography or plant cover and then mixed them to represent a single sample. To avoid possible human disturbances, the soil sampling sites were distant from roads and buildings. All samples collected in the field were stored in a refrigeration container during transportation and then freeze-dried for >48 h in the laboratory. Details of all the sampling sites, including locations, sample depth and vegetation type, are listed in Table 1.

In addition, we also collected two batches of SPM samples at water depth of 1 m, 3 m, 6 m and 8 m by filtering 50 L water through a 0.7 µm Whatman GF/F filter on site in September 2017 and January 2018, respectively. SPM samples were also stored in a refrigeration container during transportation and then freeze-dried for >48 h in the laboratory. At the same time of SPM sampling, we measured water column parameters in the lake using an YSI water quality profiler.

2.3 Sample treatment and GDGT analysis

Freeze-dried soil and sediment samples were homogenized at room temperature, and accurately weighed. Each freeze-dried filter with SPM attached was cut into small pieces using a sterilized scissor. Each sample of soil, sediment and SPM was placed in a 50 mL tube and then ultra-sonicated successively with dichloromethane/methanol (DCM/MeOH, 1:1, v/v) four times. After centrifugation

and combination of all the extracts of a sample, an internal standard consisting of synthesized C₄₆ GDGT was added with a known amount (Huguet et al., 2006). Subsequently, the total extracts were concentrated using a vacuum rotary evaporator. The nonpolar and polar fractions in the extracts were separated via silica gel column chromatography, using pure *n*-hexane and DCM/MeOH (1:1, v/v), respectively. The polar fraction containing GDGTs was dried in a gentle flow of N₂, dissolved in *n*-hexane/ethyl acetate (EtOA) (84:16, v/v) and filtered through a 0.45 µm polytetrafluoroethylene filter before instrumental analysis. We performed GDGT analysis by high performance liquid chromatography-atmospheric pressure chemical ionization-mass spectrometry (HPLC-APCI-MS; Agilent 1200 series 6460 QQQ). Following the method of Yang et al. (2015), the separation of 5- and 6-methyl brGDGTs was achieved using two silica columns in tandem (150 mm × 2.1 mm, 1.9 µm, Thermo Finnigan; U.S.A.) maintained at 40 °C. The following elution gradient was used: 84/16 *n*-hexane/EtOA (A/B) to 82/18 A/B from 5 to 65 min and then to 100% B in 21 min, followed by 100% B for 4 min to wash the column and then back to 84/16 A/B to equilibrate it for 30 min. The flow rate was at a constant 0.2 ml/min throughout. BrGDGTs were ionized and detected with single ion monitoring (SIM) at *m/z* 1050, 1048, 1046, 1036, 1034, 1032, 1022, 1020, 1018 and 744. The brGDGTs were quantified from comparing retention time and peak areas with the C₄₆ GDGT internal standard. Based on duplicate HPLC/MS analyses, the analytical errors of both the MBT'_{5ME} and MBT'_{6ME} index were ±0.01 units.

177 2.4 Calculation of GDGT-related Proxies

178 The MBT'_{5ME} and MBT'_{6ME} index were calculated following Eq. (1) and (2) as in De Jonge et al.
179 (2014):

$$180 \text{MBT}'_{5\text{ME}} = (\text{Ia} + \text{Ib} + \text{Ic}) / (\text{Ia} + \text{Ib} + \text{Ic} + \text{IIa} + \text{IIb} + \text{IIc} + \text{IIIa}) \quad (1)$$

$$181 \text{MBT}'_{6\text{ME}} = (\text{Ia} + \text{Ib} + \text{Ic}) / (\text{Ia} + \text{Ib} + \text{Ic} + \text{IIa}' + \text{IIb}' + \text{IIc}' + \text{IIIa}') \quad (2)$$

182 The isomer ratio (IR) of 6-methyl was calculated as in De Jonge et al. (2014). The $\Sigma\text{IIIa}/\Sigma\text{IIa}$ ratio was
183 calculated as in Martin et al. (2019), which is modified from Xiao et al. (2016). The weighted average
184 number of ring moieties ($\#\text{Rings}_{\text{tetra}}$, $\#\text{Rings}_{\text{penta } 5\text{ME}}$ and $\#\text{Rings}_{\text{penta } 6\text{ME}}$) followed Sinninghe Damsté
185 (2016):

$$186 \text{IR}_{6\text{ME}} = (\text{IIa}' + \text{IIb}' + \text{IIc}' + \text{IIIa}' + \text{IIIb}' + \text{IIIc}') / (\text{IIa} + \text{IIa}' + \text{IIb} + \text{IIb}' + \text{IIc} + \text{IIc}' + \text{IIIa} + \text{IIIa}' + \text{IIIb} + \\ 187 \text{IIIb}' + \text{IIIc} + \text{IIIc}') \quad (3)$$

$$188 \Sigma\text{IIIa}/\Sigma\text{IIa} = (\text{IIIa} + \text{IIIa}' + \text{IIIa}'') / (\text{IIa} + \text{IIa}') \quad (4)$$

$$189 \#\text{Rings}_{\text{tetra}} = (\text{Ic} * 2 + \text{Ib}) / (\text{Ia} + \text{Ib} + \text{Ic}) \quad (5)$$

$$190 \#\text{Rings}_{\text{penta } 5\text{ME}} = (\text{IIc} * 2 + \text{IIb}) / (\text{IIa} + \text{IIb} + \text{IIc}) \quad (6)$$

$$191 \#\text{Rings}_{\text{penta } 6\text{ME}} = (\text{IIc}' * 2 + \text{IIb}') / (\text{IIa}' + \text{IIb}' + \text{IIc}') \quad (7);$$

192 The Roman numerals represent different brGDGT homologues referred to Yang et al. (2015) and
193 Weber et al. (2015) (see [Appendix 1](#)).

194 In this study, we used two silica columns in tandem and successfully separated 5- and 6-methyl

195 brGDGTs. However, many previous brGDGT studies on lake materials used one cyano column,
196 which did not separate 5- and 6-methyl brGDGTs (e.g., Wang et al., 2012; Loomis et al., 2014; Hu et
197 al., 2015, 2016; Cao et al., 2017). In order to facilitate comparison with previous studies, we
198 reanalyzed the published brGDGT data without separation of 5- and 6-methyl brGDGTs in the
199 Gonghai Lake (Cao et al., 2017). For temperature estimations, we listed the Eqs. (8–17) used in this
200 study in Table 2.

201

202 **3 Results**

203 **3.1 Seasonal changes in environmental parameters**

204 The AT in our study area ranged from -12.2 to 21.6 °C, below freezing in winter (November to
205 February) and at 4.3 °C for the mean in the year 2018 (Fig. 1c). Surface LWT ranged from 3.4 to
206 21.9 °C (average 10.6 °C), and remained stable at ca. 4 °C in winter (Fig. 1c). In September 2017,
207 water column stratification was weak with temperature ranging from 16.9 to 17.8 °C and exhibiting a
208 gradual and slight decrease with depth (Fig. 2). In January 2018, the lake surface water was frozen
209 and LWTs under ice were 4 °C at all depths (Fig. 2).

210 **3.2 Concentration and distribution of brGDGTs**

211 BrGDGTs were detected in all samples, and their total concentration ranged between 16 – 75 ng/g
212 dry weight (dw) in surface soils from Gonghai catchment, 42 – 707 ng/g dw in lake surface sediments,

213 5–10 ng/l in September and 3–8 ng/l in January in water SPM (Table 1 and Fig. 2). The average
214 content of brGDGTs in lake surface sediments (291 ng/g dw) was significantly higher than in surface
215 soils (31 ng/g dw) and particularly exhibited an increasing trend with water depth. In SPM, the
216 average concentration of brGDGTs in water column showed no significant difference between
217 September and January ($t = 1.2$, $p = 0.26$) but there was a clearer trend of increase with depth in
218 September than in January (Fig. 2). Notably, the compound IIIa", which was regarded typical for in
219 situ produced lacustrine brGDGTs (Weber et al., 2015), was also identified in the Gonghai Lake
220 sediments and SPM but not found in catchment soils (Table1 and Fig. 3a). There was no significant
221 difference in average concentration of IIIa" in water column between September and January ($t = 0.62$,
222 $p = 0.28$). The change patterns of IIIa" with water depth in SPM and sediments were the same as those
223 of the total brGDGTs (Table 1).

224 The brGDGTs in soils, sediments and SPM were dominated by brGDGT II and III series, with
225 acyclic compounds dominant in every series (Fig. 3a). In comparison, the mean $\Sigma\text{IIIa}/\Sigma\text{IIa}$ ratio value
226 in sediments (1.14–1.52 range, 1.30 average) was higher than in SPM (0.84–1.11 range, 0.99 average)
227 and soils (0.56–0.86 range, 0.70 average). In addition, 6-methyl brGDGTs dominated over 5-methyl
228 brGDGTs in soils, exhibiting mean $\text{IR}_{6\text{ME}}$ of 0.62; whereas the two isomers were similar in content in
229 sediments ($\text{IR}_{6\text{ME}} = 0.47\text{--}0.60$ range, 0.51 average) and SPM ($\text{IR}_{6\text{ME}} = 0.45\text{--}0.50$ range, 0.48 average)
230 (Fig. 3a).

231 3.3 Cyclisation ratio, methylation index of brGDGTs

232 The #Rings_{tetra} values varied from 0.26 to 0.45 (0.36 average) in catchment soils, 0.37–0.43 (0.40
233 average) in September and 0.39–0.42 (0.40 average) in January in SPM, and 0.45–0.47 (0.45 average)
234 in surface sediments (Fig. 3b). The #Rings_{penta 5ME} showed the same increasing trend as #Rings_{tetra}
235 from soils to SPM and then to sediments (Fig. 3b). In contrast, #Rings_{penta 6ME} in soils was similar to
236 that in sediments and SPM (Fig. 3b).

237 The MBT'_{5ME} values varied from 0.31 to 0.36 (average 0.35) in catchment soils, 0.23–0.29 (0.26
238 average) in surface sediments, 0.23–0.28 (0.26 average) in September and 0.24–0.26 (0.25 average) in
239 January in SPM (Fig. 3b). Generally, the MBT'_{5ME} exhibited decreasing trends with water depth in
240 surface sediments and SPM in September (Fig. 2). The MBT'_{6ME} values varied from 0.20 to 0.33 (0.25
241 average) in surface soils of the lake catchment, 0.22–0.27 (0.25 average) in surface sediments,
242 0.24–0.32 (0.28 average) in September and 0.26–0.28 (0.27 average) in January in SPM (Fig. 3b). The
243 MBT'_{6ME} also decreased in SPM in September, but increased in sediments with water depth. Both
244 MBT'_{5ME} and MBT'_{6ME} changed less in SPM in January with water depth (Fig. 2).

245

246 4 Discussions

247 4.1 In situ production of brGDGTs in the Gonghai Lake

248 Although brGDGTs have a strong potential to record temperature in lacustrine regions (Tierney

249 et al., 2010; Pearson et al., 2011; Sun et al., 2011; Loomis et al., 2012; Dang et al., 2018; Russell et al.,
250 2018), the sources of brGDGTs in lake sediments should be carefully identified. There are two
251 potential sources, including allochthonous input from soil and autochthonous production in lake water
252 and/or surface sediments, which can be distinguished by comparison of brGDGT distribution between
253 surface sediments and soils (Tierney and Russell, 2009; Loomis et al., 2011; Wang et al., 2012; Hu et
254 al., 2015; Sinninghe Damsté, 2016).

255 In the Gonghai Lake, the average content of brGDGTs in surface sediments was significantly
256 higher than that in surface soils (Table 1). Moreover, they exhibited a clearly increasing trend with
257 water depth, suggesting a possible autochthonous contribution, even though soil brGDGTs input
258 cannot be ignored. Moreover, the brGDGT distribution in surface sediments was similar to that of
259 SPM, but quite different from that of soils (Fig. 3a). Several lines of evidence indicate a substantial in
260 situ production of brGDGTs in the Gonghai Lake. (I) The presence of IIIa" in the Gonghai Lake
261 sediments and SPM but the absence in the catchment soils may be a direct evidence of in situ
262 production in the lake (Fig. 3a). A similar conclusion has been drawn in a Swiss mountain lake basin
263 (Weber et al., 2015). (II) In the Gonghai Lake, the $\Sigma\text{IIIa}/\Sigma\text{IIa}$ ratio in sediments (1.3 average) and
264 SPM (0.99 average) were much higher than in catchment soils (0.7 average) (Fig. 3a). The values of
265 $\Sigma\text{IIIa}/\Sigma\text{IIa} > 0.92$ has been regarded as the evidence of aquatic production in previous reports (Xiao et
266 al., 2016; Martin et al., 2019; Zhang et al., 2020). (III) The average values of $\text{IR}_{6\text{ME}}$ in surface

267 sediments and SPM were significantly lower than in catchment soils (Fig. 3a), suggesting at least
268 some of 5-methyl brGDGTs in lake sediments and SPM were produced in situ. (IV) The cyclisation
269 ratio of brGDGTs has been also used to distinguish the aquatic production, although applied to marine
270 sediments, from soil input (Sinninghe Damsté, 2016). In the Gonghai Lake, #Rings_{tetra} and #Rings_{penta}
271 _{5ME} were clearly higher in sediments than in catchment soils ($p < 0.05$ for #Rings_{tetra}, $p < 0.01$ for
272 #Rings_{penta 5ME}), although #Rings_{penta 6ME} in sediments was similar to that in catchment soils ($p = 0.11$
273 for #Rings_{penta 6ME}; Fig. 3b).

274 The in situ production of brGDGTs in the Gonghai Lake can be also evidenced by the
275 discrepancies in reconstructed temperatures between soils and sediments/SPM. Based on the new
276 global soil calibration of Eq. (9) and regional soil calibration of Eq. (10) for China, the
277 brGDGT-derived AT in the Gonghai catchment soils ranged from 1.18 to 2.75 °C (average $2.33 \pm$
278 0.65 °C; Table 1) and from -4.22 to -1.21 °C (average -2.42 ± 1.19 °C; Table 1), respectively.
279 Considering the ± 4.8 °C uncertainty of the global calibration and ± 2.5 °C of the regional calibration,
280 the estimated temperatures from the global calibration are much close to the mean annual AT of
281 4.3 °C, thereby well reflecting mean annual AT in our study lake catchment. Then, the global
282 calibration Eq. (9) was applied to sediment/SPM data, yielding estimated temperatures $-0.50 \pm$
283 0.78 °C in surface sediments and -0.55 ± 0.52 °C in SPM and hence much lower than those from
284 surface soils (2.33 ± 0.65 °C; Table 1). Similarly, temperature underestimation using soil-derived

285 calibration has been widely reported in many modern lake sediments (e.g., Tierney et al., 2010;
286 Loomis et al., 2012; Pearson et al., 2011; Russell et al., 2018), which has been attributed to in situ
287 production of brGDGTs in the lakes.

288 **4.2 Lacustrine brGDGT-derived ATs are warm season biased (average monthly** 289 **temperature >0 °C)**

290 The suggested in situ production of brGDGTs prompts us to use lake-specific temperature
291 calibrations (Tierney et al., 2010; Pearson et al., 2011; Sun et al., 2011; Loomis et al., 2012; Dang et
292 al., 2018; Russell et al., 2018) to reconstruct AT, although not differentiated quantitatively the relative
293 contributions of aquatic vs. soil-derived brGDGTs. Here, we applied four equations, Eqs. (11) and
294 (15)–(17) in Table 2, to our sedimentary brGDGT data.

295 As shown in Fig. 4a, the reconstructed temperatures using different equations are >6.4 °C.
296 Despite discrepancies in the temperature values between calibrations, they are comparable
297 considering the uncertainty of each calibration. A prominent feature of the reconstructed temperature
298 is that they, especially those in the shallower sediments, are well above the annual mean AT but more
299 close to the mean warm season AT (average monthly temperature >0 °C). This feature is consistent
300 with numerous studies proposing that lacustrine brGDGT-derived ATs are warm season biased
301 (Shanahan et al., 2013; Peterse et al., 2014; Dang et al., 2018).

302 Many previous brGDGT instrumental analyses on lake materials used one cyano column, which

303 did not separate 5- and 6-methyl brGDGTs. Using the data published in the same lake from Cao et al.
304 (2017), we re-calculated temperature using different calibrations. The results showed that the absolute
305 temperature estimates were all significantly warmer than the mean annual AT (Table 3), with the
306 temperature offsets varying from 4–10 °C, which cannot be fully explained by the uncertainty of each
307 calibration. Therefore, it appears that sedimentary brGDGT-derived temperature is warm season
308 biased in the Gonghai Lake irrespective of whether or not 5- and 6-methyl brGDGTs are separated.

309 Moreover, we found the warm season bias of reconstructed AT is increasingly apparent with the
310 increase of latitude. Here, five lakes, including Lower King pond (Loomis et al., 2014), Qinghai Lake
311 (Wang et al., 2012), Lake Donghu (Qian et al., 2019), Huguangyan maar (Hu et al., 2015, 2016) and
312 Lake Towuli (Tierney and Russell, 2009), were selected to compare as an example. These lakes are
313 located in different regions spanning a relatively large environmental gradient, and more importantly,
314 brGDGT data from both the lake surface sediments and the surrounding soils are available. We
315 re-calculated temperatures from published data of brGDGTs from these lakes (Fig. 5) by applying the
316 calibration of global soils (Eq (8); Peterse et al., 2012) to the surrounding soils and the calibration of
317 lake surface sediments (Eq (11); Sun et al., 2011) to the lake sediments. As shown in Fig. 5a, the
318 brGDGT-inferred temperatures in catchment soils are similar to local mean annual ATs. In contrast,
319 the brGDGT-inferred temperatures in lake sediments are similar to the local mean annual ATs only in
320 low-latitude lakes, whereas they become increasingly higher than the local mean annual ATs toward

321 higher latitudes (Fig. 5b). In comparison, the brGDGT-inferred temperatures are close to the local
322 mean ATs in warm season (average monthly mean AT $>0^{\circ}\text{C}$) in all these lakes (Fig. 5c). Besides
323 above discussed lakes, some investigations have also pointed out that brGDGT-inferred temperatures
324 are higher than mean annual AT, close to warm season AT or summer AT in mid- and high-latitude
325 lakes (Shanahan et al., 2013; Peterse et al., 2014; Foster et al., 2016; Dang et al., 2018), but close to,
326 or lower than, mean annual AT in low-latitude lakes (Tierney et al., 2010; Loomis et al., 2012).
327 Therefore, it is a global occurrence that sedimentary brGDGT-derived temperatures are warm season
328 biased in lakes at cold regions.

329 4.3. Lacustrine brGDGTs reflect deep/bottom water temperature

330 Another feature of sedimentary brGDGT-derived ATs in our results is that there is a consistently
331 decreasing trend of reconstructed temperature with depth using Eqs. (11), (15) and (16) (Fig. 4a),
332 albeit less clear using Eq. (15). It is not understandable that AT is correlated with water depth.
333 Interestingly, both $\text{MBT}'_{5\text{ME}}$ and $\text{MBT}'_{6\text{ME}}$ in SPM showed decreasing trends with water depth in
334 September, similar to the water temperature profile of the month (Fig. 2). In January, the relatively
335 unchanged $\text{MBT}'_{5\text{ME}}$ and $\text{MBT}'_{6\text{ME}}$ (<0.02) also mirror the constant water temperature of the month
336 (Fig. 2). Accordingly, we surmise that brGDGT-derived temperatures in sediments and SPM may
337 actually reflect water temperature.

338 Although the $\text{MBT}'_{5\text{ME}}$ and $\text{MBT}'_{6\text{ME}}$ in SPM in the lake seem to reflect temperature changes in

the water column to some extent, the differences of brGDGT-derived temperatures based on lake-specific calibrations between September and January (-0.93 to 1.21 °C) are much lower than the measured difference (~ 13 °C), independent of the calibration of (15), (16) or (17) (Tables 1 and 2). In fact, similar results have been also reported in other lakes. For example, in the Lower King Pond, the calculated seasonal temperature difference in surface water SPM was 5.4 °C, significantly smaller than the measured difference about 28.3 °C (Loomis et al., 2014); in the Huguangyan maar lake, the calculated seasonal temperature difference was 8 °C, also significantly smaller than the measured difference about 16 °C (Hu et al., 2016). The reduced seasonal contrasts in SPM brGDGT-derived temperatures could result from the existence of “fossil” brGDGTs and sediment resuspension in the water column, which may lead to a long (e.g., multi seasonal) residence time of SPM, although not exactly known (Loomis et al., 2014). The even smaller differences in MBT'_{5ME} and MBT'_{6ME} between sediments and SPM at deeper sites in our results (Fig. 2) suggest the impacts of sediment suspension on SPM. Such a scenario may lead to more “fossil” brGDGTs in SPM than those produced within a specific season or month, as evidenced by an observation showing that only a small proportion of intact polar lipid of brGDGTs, indicative of fresh brGDGTs, was detected in total brGDGTs in SPM in a shallow lake (Qian et al., 2019). Besides, several parameters, such as $\Sigma IIIa/\Sigma IIa$, IR_{6ME} , $\#Rings_{tetra}$ and $\#Rings_{penta}$ in SPM were in-between the soil and sediment values, we speculate terrestrial inputs may be a factor, if any, to reduce the seasonal changes of brGDGTs in SPM.

In addition to reflecting water temperature, the decrease trend with depth in sedimentary brGDGT-derived temperature further suggests a controlling influence of deep/bottom water temperature. Similar occurrence has been observed also in Lower King pond in temperate northern Vermont, U.S.A. and Lake Biwa in central Japan, showing that the sedimentary brGDGT-derived temperatures decreased with water depth, co-varied with mean annual LWT at depths (Ajiako et al., 2014; Loomis et al., 2014). Also in Loch Lomond in the UK, the brGDGT-derived temperatures by different MBT/CBT lacustrine calibrations all decreased with water depth (Buckles et al., 2014b). So, a water depth-related production of brGDGTs should be considered when interpreting brGDGT-derived temperatures, which will be discussed below.

We notice recent works suggesting that changes in microbial community composition may be responsible for variations in the distribution of brGDGTs, causing the different responses of soil brGDGTs temperature, as well as pH, under different temperature ranges (e.g., De Jonge et al. 2019). However, little is known about whether this idea is applicable to aquatic environments. According to De Jonge et al. (2019), community change can be indicated by the community index (CI = Community Index) in soils, with $CI > 0.64$ indicating warm community cluster and $CI < 0.64$ indicating cold community cluster. Here we applied the CI to lake sediment data including ours and those available for the entire 15 brGDGT compounds in literature, mostly from the east Africa. As shown in Fig. 4b, the putative two community clusters also occur in lake environments, with the

Gonghai community belonging to the “cold” cluster. Different from soil data showing that MBT'_{5ME} captures large temperature changes only when the bacterial community shows a strong change in composition (De Jonge et al. 2019), it seems that MBT'_{5ME} changes linearly with LWT, which is less influenced by the bacterial community change (Fig. 4b). However, we note that the test of community change here is rather crude, and further studies on the biological sources of brGDGT and their response to temperature in aquatic environments are needed.

4.4 Ice cover formation as a mechanism for the apparent warm bias of lacustrine brGDGT-derived temperature

One explanation for the warm season biases of the lacustrine brGDGT-derived temperature in mid to high latitudes has been proposed as the excessive production of brGDGTs during the warm/summer season relative to winter season (Pearson et al., 2011; Shanahan et al., 2013; Peterse et al., 2014; Foster et al., 2016; Dang et al., 2018). In the Gonghai Lake, the average concentration of brGDGTs in SPM is 7.1 ± 2.0 ng/l in September and 5.2 ± 2.3 ng/l in January (Fig. 2) with no significant difference. Besides, the compound IIIa", which is likely specifically of aquatic origin (Weber et al., 2015), also showed no significant seasonal difference (0.36 ± 0.09 ng/l in September vs. 0.31 ± 0.15 ng/l in January). More importantly, the small differences in MBT'_{5ME} and MBT'_{6ME} of SPM and their derived temperatures between September and January suggest that the actual seasonal temperature difference, which may be recorded by the immediately produced brGDGTs, would have

393 been substantially masked or smoothed by the predominance of fossil brGDGTs. In addition,
394 brGDGT-derived temperatures in SPM were close to mean annual water temperature and lower than
395 the mean annual warm water temperature, also did not support the excessive production of brGDGTs
396 during the warm/summer season relative to winter season. Besides, the season of higher brGDGT
397 concentration has been found different in different lakes, e.g., in spring and autumn in Lower King
398 pond (Loomis et al., 2014), in winter in Lake Lucerne (Blaga et al., 2011), and in summer in Lake
399 Donghu in central China (Qian et al., 2019). However, in all these lakes in temperate climate zones,
400 the brGDGT-derived temperatures have been found to be slightly or significantly warm season biased
401 (Loomis et al., 2014; Qian et al., 2019; Fig. 5b). The above evidence suggests that other factors, other
402 than seasonality in the production of brGDGTs in the lakes, should be responsible for the bias of
403 brGDGT-inferred temperature toward warm season in higher latitudes (Fig. 5b and c).

404 The brGDGT-derived temperature in lake sediments could be influenced by the vertically
405 inhomogeneous production of brGDGTs with maximum in deep/bottom waters. This seems true in the
406 Gonghai Lake as evidenced by the increase of sedimentary brGDGT content and the decrease of
407 brGDGT-derived temperature with water depth as discussed above. The bio-precursors of brGDGTs
408 have been proposed to be bacteria with an anaerobic heterotrophic lifestyle (Sinninghe Damsté et al.,
409 2000; Weijers et al., 2006b, 2010; Weber et al., 2015, 2018), implying that a potentially anoxic
410 (micro)environment in deep/bottom water favors the production of brGDGTs (Woltering et al., 2012;

411 Zhang et al., 2016; Weber et al., 2018). Such an occurrence could lead to higher proportion of ‘colder
412 temperature’ brGDGTs in lake sediments, which may at least partly interpret the frequently observed
413 cool bias of brGDGT-derived temperatures in many lakes, such as the Lake Challa, Lake Albert, Lake
414 Edward and Lake Tanganyika (Tierney et al., 2010; Loomis et al., 2012; Buckles et al., 2014a). The
415 MBT/CBT-derived temperature in the tropical Lake Huguangyan was thought to reflect mean annual
416 AT (Hu et al., 2015, 2016); however, has recently been proposed to be winter/cool biased (Chu et al.,
417 2017). We suppose that, as a monomictic lake, the lower mean annual temperature than mean annual
418 AT in deep/bottom waters might be a cause for the cool biased brGDGT temperature in the lake.
419 Intriguingly, all the above lakes are in the tropics. Nonetheless, the deep/bottom water bias may be
420 still true for the brGDGT-derived temperature in lakes in higher latitude, as suggested by our data in
421 the Gonghai Lake. However, different from those tropical lakes, in higher-latitude lakes, including the
422 Gonghai Lake (this study), Qinghai Lake (Wang et al., 2012), Lower King pond (Loomis et al., 2014),
423 some cold-region lakes in China (Dang et al., 2018) and some Arctic lakes (Shanahan et al., 2013;
424 Peterse et al., 2014), the sedimentary brGDGT-derived temperatures are all higher, not lower, than the
425 mean annual AT. Therefore, more production of brGDGTs in deep/bottom water alone is not
426 responsible for the warm bias of brGDGT-derived temperature in surface sediments at least in these
427 lakes.

428 Although brGDGTs in lake sediments were confirmed to be mainly derived from in situ aquatic

production, previous studies deemed that the estimated temperatures can still reflect AT by assuming that LWT is tightly coupled with AT (Tierney et al., 2010). In fact, such tight coupling can be found in tropical-subtropical lakes, where AT is always above the freezing point, but is not true in higher-latitude lakes such as Lower King pond and Gonghai Lake with lake surface freezing in winter (Fig. 6a and b). The reason is that lake surface ice prevents the thermal exchange between water and air, leading to decoupling between LWT (usually ≥ 4 °C) and AT (< 0 °C) in winter in cold regions. The decoupling makes mean annual LWT, even at the deep/bottom waters, higher than mean annual AT. Therefore, the greater warm biases of brGDGT-derived temperatures from surface sediments in higher latitudes (Fig. 5b) could be due to the stronger decoupling (e.g., longer freezing time) between LWT and AT. Nevertheless, annual mean LWT appears basically close to the mean AT in warm season (average monthly temperature > 0 °C) (Fig. 6f), which could be the reason why the brGDGT-inferred temperatures are similar to the mean warm season AT (Fig. 5c). Due to lack of detailed AT and LWT data in literature, we failed to show more examples than as shown in Fig. 6, especially those from even higher latitudes. However, we proposed a simple model for the relationship between LWT and AT in a year cycle (Fig. 7), which may be a universal physical phenomenon in shallow lakes. In the mid- and high-latitude region, we believe the decoupling between AT and LWT caused by ice formation in winter may be applied to explain the observed seasonality of the brGDGT temperature records. For example, the biases of brGDGT-derived temperatures toward summer AT observed

extensively in the Arctic and Antarctic lakes (Shanahan et al., 2013; Foster et al., 2016) are compatible with the mechanism that we propose here. Of course, considering limited data in this study, more investigations are needed to test our viewpoint in future studies.

5 Conclusions

We investigated the brGDGT distribution in catchment soils, surface sediments and water column SPM in September and January in the Gonghai Lake in north China. The lake is characterized by ice formation on its surface and a constant 4 °C condition in the underlying water in winter. The brGDGT distribution in sediments were similar to that in SPM but differed clearly from that in soils, indicating mainly in situ production of brGDGTs in the lake. BrGDGTs in SPM showed little seasonal differences in concentration and MBT'_{SME}, likely due to a dominant contribution of fossil brGDGTs caused by, e.g., sediment suspension, which may mask any seasonal signals documented in sedimentary brGDGTs. The increase of brGDGT content and decrease of methylation index with water depth in sediments suggested more contribution of aquatic brGDGTs produced from deep/bottom waters. Based on available lake calibrations, we found that the temperature estimates in surface sediments and SPM of the Gonghai Lake were higher than the measured mean annual AT but close to warm season AT, which cannot interpreted by more aquatic production of brGDGTs in warm season and/or in deep/bottom waters. We found that such a warm biased brGDGT-derived temperature

465 was actually close to the mean annual LWT, and therefore proposed that water-air temperature
466 decoupling due to ice formation at the lake surface in winter, which can prevent thermal exchange
467 between lake water and air, may be the cause for the apparent bias toward warm AT of lacustrine
468 brGDGT-derived temperatures. Since the warm AT bias of brGDGT estimates has been observed
469 extensively in mid- and high-latitude shallow lakes, we believe the mechanism proposed here could
470 also be applicable to these lakes.

471

472 **Data availability**

473 The raw data of this study can be accessed from <https://figshare.com/s/a4f324247ecd9d1ac575>.

474 **Author contribution**

475 ZR designed experiments, FS and JC collected samples and JC carried experiments out. JC, GJ and
476 ZR prepared the manuscript with contributions from all co-authors.

477 **Conflicts of interest**

478 The authors declare that they have no conflict of interest.

479

480 **Acknowledgments**

481 The work was supported by the Hunan Provincial Natural Science foundation of China (2018JJ1017),
482 the National Natural Science Foundation of China (41772373), and the Fundamental Research Funds

483 for the Central Universities of China (grant no. lzujbky-2018-it77). Two anonymous reviewers are
484 thanked for their valuable comments.

485

486 **References**

487 Ajioka, T., Yamamoto, M., and Murase, J.: Branched and isoprenoid glycerol dialkyl glycerol
488 tetraethers in soils and lake/river sediments in Lake Biwa basin and implications for MBT/CBT
489 proxies, *Org. Geochem.*, 73, 70-82, doi: 10.1016/j.orggeochem.2014.05.009, 2014.

490 Bechtel, A., Smittenberg, R. H., Bernasconi, S. M., and Schubert, C. J.: Distribution of branched and
491 isoprenoid tetraether lipids in an oligotrophic and a eutrophic Swiss lake: Insights into sources
492 and GDGT-based proxies, *Org. Geochem.*, 41, 822-832, doi:10.1016/j.orggeochem.2010.04.022,
493 2010.

494 Blaga, C. I., Reichart, G. J., Heiri, O., and Sinninghe Damsté, J. S.: Tetraether membrane lipid
495 distributions in water-column particulate matter and sediments: a study of 47 European lakes
496 along a north-south transect, *J. Paleolimnol.*, 41, 523-540, doi:10.1007/s10933-008-9242-2,
497 2009.

498 Blaga, C. I., Reichart, G. J., Schouten, S., Lotter, A. F., Werne, J. P., Kosten, S., Mazzeo, N., Lacerot,
499 G., and Sinninghe Damsté, J. S.: Branched glycerol dialkyl glycerol tetraethers in lake sediments:
500 can they be used as temperature and pH proxies, *Org. Geochem.*, 41, 1225-1234,

doi:10.1016/j.orggeochem.2010.07.002, 2010.

Blaga, C. I., Reichart, G. J., Vissers, E. W., Lotter, A. F., Anselmetti, F. S., and Sinninghe Damsté, J. S.: Seasonal changes in glycerol dialkyl glycerol tetraether concentrations and fluxes in a perialpine lake: Implications for the use of the TEX86 and BIT proxies, *Geochim. Cosmochim. Acta*, 75, 6416-6428, doi:10.1016/j.gca.2011.08.016, 2011.

Buckles, L. K., Weijers, J. W. H., Verschuren, D., and Sinninghe Damsté, J. S.: Sources of core and intact branched tetraether membrane lipids in the lacustrine environment: Anatomy of Lake Challa and its catchment, equatorial East Africa, *Geochim. Cosmochim. Acta*, 140, 106-126, doi:10.1016/j.gca.2014.04.042, 2014a.

Buckles, L. K., Weijers, J. W. H., Tran, X. M., Waldron, S., and Sinninghe Damsté, J. S.: Provenance of tetraether membrane lipids in a large temperate lake (Loch Lomond, UK): implications for glycerol dialkyl glycerol tetraether (GDGT)-based palaeothermometry, *Biogeosciences*, 11, 5539-5563, doi:10.5194/bg-11-5539-2014, 2014b.

Cao, J. T., Rao, Z. G., Jia, G. D., Xu, Q. H., and Chen, F. H.: A 15 ka pH record from an alpine lake in north China derived from the cyclization ratio index of aquatic brGDGTs and its paleoclimatic significance, *Org. Geochem.*, 109, 31-46, doi:10.1016/j.orggeochem.2017.02.005, 2017.

Chen, F. H., Yu, Z. C., Yang, M. L., Ito, E., Wang, S. M., Madsen, D. B., Huang, X. Z., Zhao, Y., Sato, T., John, B. B. H., Boomer, I., Chen, J. H., An, C. B., and Wünnemann, B.: Holocene moisture

evolution in arid central Asia and its out-of-phase relationship with Asian monsoon history, *Quat. Sci. Rev.*, 27, 351-364, doi:10.1016/j.quascirev.2007.10.017, 2008.

Chen, F. H., Liu, J. B., Xu, Q. H., Li, Y. C., Chen, J. H., Wei, H. T., Liu, Q. S., Wang, Z. L., Cao, X. Y. and Zhang, S. R.: Environmental magnetic studies of sediment cores from Gonghai Lake: implications for monsoon evolution in North China during the late glacial and Holocene, *J. Paleolimnol.*, 49, 447-464, doi:10.1007/s10933-012-9677-3, 2013.

Chen, F. H., Xu, Q. H., Chen, J. H., Birks, H. J. B., Liu, J. B., Zhang, S. R., Jin, L. Y., An, C. B., Telford, R. J., Cao, X. Y., Wang, Z. L., Zhang, X. J., Selvaraj, K., Lu, H. Y., Li, Y. C., Zheng, Z., Wang, H. P., Zhou, A. F., Dong, G. H., Zhang, J. W., Huang, X. Z., Bloemendal, J. and Rao, Z. G.: East Asian summer monsoon precipitation variability since the last deglaciation, *Sci. Rep.*, 5, 11186, doi:10.1038/srep11186, 2015.

Chu, G., Sun, Q., Zhu, Q., Shan, Y., Shang, W., Ling, Y., Su, Y., Xie, M., Wang, X., Liu, J.: The role of the Asian winter monsoon in the rapid propagation of abrupt climate changes during the last deglaciation, *Quat. Sci. Rev.*, 177, 120-129, doi:10.1016/j.quascirev.2017.10.014, 2017.

Dang, X. Y., Ding, W. H., Yang, H., Pancost, R. D., Naafs, B. D. A., Xue, J. T., Lin, X., Lu, J. Y., and Xie, S. C.: Different temperature dependence of the bacterial brGDGT isomers in 35 Chinese lake sediments compared to that in soils, *Org. Geochem.*, 119, 72-79, doi:10.1016/j.orggeochem.2018.02.008, 2018.

537 De Jonge, C., Hopmans, E.C., Stadnitskaia, A., Rijpstra, W. I. C., Hofland, R., Tegelaar, E., Sinninghe
 538 Damsté, J.S.: Identification of novel penta- and hexamethylated branched glycerol dialkyl
 539 glycerol tetraethers in peat using HPLC-MS², GC-MS and GC-SMB-MS, *Org. Geochem.*, 54,
 540 78-82, doi:10.1016/j.orggeochem.2012.10.004, 2013.

541 De Jonge, C., Hopmans, E. C., Zell, C. I., Kim, J. H., Schouten, S., and Sinninghe Damsté, J. S.:
 542 Occurrence and abundance of 6-methyl branched glycerol dialkyl glycerol tetraethers in soils:
 543 implications for palaeoclimate reconstruction, *Geochim. Cosmochim. Acta*, 141, 97-112,
 544 doi:10.1016/j.gca.2014.06.013, 2014.

545 De Jonge, C., Radujković, D., Sigurdsson, B. D., Weedon, J. T., Janssens, I., Peterse, F.: Lipid
 546 biomarker temperature proxy responds to abrupt shift in the bacterial community composition in
 547 geothermally heated soils, *Org. Geochem.*, 137, 103897, doi:10.1016/j.orggeochem.2019.07.006.

548 Deng, L. H., Jia, G. D., Jin, C. F., and Li, S. J.: Warm season bias of branched GDGT temperature
 549 estimates causes underestimation of altitudinal lapse rate, *Org. Geochem.*, 96, 11-17,
 550 doi:10.1016/j.orggeochem.2016.03.004, 2016.

551 Foster, L. C., Pearson, E. J., Juggins, S., Hodgson, D. A., Saunders, K. M., Verleyen, E., and Roberts,
 552 S. J.: Development of a regional glycerol dialkyl glycerol tetraether (GDGT)-temperature
 553 calibration for Antarctic and sub-Antarctic lakes, *Earth Planet. Sci. Lett.*, 433, 370-379,
 554 doi:10.1016/j.epsl.2015.11.018, 2016.

555 Hopmans, E. C., Weijers, J. W. H., Schefuß, E., Herfort, L., Sinninghe Damsté, J. S., and Schouten, S.:
 556 A novel proxy for terrestrial organic matter in sediments based on branched and isoprenoid
 557 tetraether lipids, *Earth Planet. Sci. Lett.*, 224, 107-116, doi:10.1016/j.epsl.2004.05.012, 2004.

558 Hu, J. F., Zhou, H. D., Peng, P. A., Yang, X. P., Spiro, B., Jia, G. D., Wei, G. J. and Ouyang, T. P.:
 559 Reconstruction of a paleotemperature record from 0.3-3.7 ka for subtropical South China using
 560 lacustrine branched GDGTs from Huguangyan Maar, *Paleogeogr. Paleoclimatol. Paleoecol.*, 435,
 561 167-176, doi:10.1016/j.palaeo.2015.06.014, 2015.

562 Hu, J. F., Zhou, H. D., Peng, P. A., and Spiro, B.: Seasonal variability in concentrations and fluxes of
 563 glycerol dialkyl glycerol tetraethers in Huguangyan Maar Lake, SE China: Implications for the
 564 applicability of the MBT-CBT paleotemperature proxy in lacustrine settings, *Chem. Geol.*, 420,
 565 200-212, doi:10.1016/j.chemgeo.2015.11.008, 2016.

566 Huguet, C., Hopmans, E. C., Febo-Ayala, W., Thompson, D. H., Sinninghe Damsté, J. S., and
 567 Schouten, S.: An improved method to determine the absolute abundance of glycerol dibiphytanyl
 568 glycerol tetraether lipids, *Org. Geochem.*, 37, 1036-1041,
 569 doi:10.1016/j.orggeochem.2006.05.008, 2006.

570 Li, X. M., Wang, M. D., Zhang, Y. Z., Lei, L., and Hou, J. Z.: Holocene climatic and environmental
 571 change on the western Tibetan Plateau revealed by glycerol dialkyl glycerol tetraethers and leaf
 572 wax deuterium-to-hydrogen ratios at Aweng Co, *Quaternary Res.*, 87, 455–467,

doi:10.1017/qua.2017.9, 2017.

Loomis, S. E., Russell, J. M., and Sinninghe Damsté, J. S.: Distributions of branched GDGTs in soils and lake sediments from western Uganda: implications for a lacustrine paleothermometer, *Org. Geochem.*, 42, 739-751, doi:10.1016/j.orggeochem.2011.06.004, 2011.

Loomis, S. E., Russell, J. M., Ladd, B., Street-Perrott, F. A., and Sinninghe Damsté, J. S.: Calibration and application of the branched GDGT temperature proxy on East African lake sediments, *Earth Planet. Sci. Lett.*, 357-358, 277-288, doi:10.1016/j.epsl.2012.09.031, 2012.

Loomis, S. E., Russell, J. M., Heurreux, A. M., Andrea, W. J. D., and Sinninghe Damsté, J. S.: Seasonal variability of branched glycerol dialkyl glycerol tetraethers (brGDGTs) in a temperate lake system, *Geochim. Cosmochim. Acta*, 144, 173-187, doi:10.1016/j.gca.2014.08.027, 2014.

Martin, C., Ménot, G., Thouveny, N., Davtian, N., Andrieu-Ponel, V., Reille, M., and Bard, E.: Impact of human activities and vegetation changes on the tetraether sources in Lake St Front (Massif Central, France), *Org. Geochem.*, 135, 38–52, doi:10.1016/j.orggeochem.2019.06.005, 2019.

Naeher, S., Peterse, F., Smittenberg, R. H., Niemann, H., Zigah, P. K., and Schubert, C. J.: Sources of glycerol dialkyl glycerol tetraethers (GDGTs) in catchment soils, water column and sediments of Lake Rotsee (Switzerland)-implications for the application of GDGT-based proxies for lakes, *Org. Geochem.*, 66, 164-173, doi:10.1016/j.orggeochem.2013.10.017, 2014.

Naafs, B. D. A., Gallego-Sala, A. V., Inglis, G. N., and Pancost, R. D.: Refining the global branched

glycerol dialkyl glycerol tetraether (brGDGT) soil temperature calibration, *Org. Geochem.*, 106,
48-56, doi:10.1016/j.orggeochem.2017.01.009, 2017.

Niemann, H., Stadnitskaia, A., Wirth, S. B., Gilli, A., Anselmetti, F. S., Sinninghe Damsté, J. S.,
Schouten, S., Hopmans, E. C., and Lehmann, M. F.: Bacterial GDGTs in Holocene sediments
and catchment soils of a high Alpine lake: application of the MBT/CBT-paleothermometer, *Clim.*
Past, 8, 889-906, doi:10.5194/cp-8-889-2012, 2012.

Ning, D. L., Zhang, E. H., Shulmeister, J., Chang, J., Sun, W. W., and Ni, Z. Y.: Holocene mean
annual air temperature (MAAT) reconstruction based on branched glycerol dialkyl glycerol
tetraethers from Lake Ximenglongtan, southwestern China, *Org. Geochem.*, 133, 65-76,
doi:10.1016/j.orggeochem.2019.05.003, 2019.

Pearson, E. J., Juggins, S., Talbot, H. M., Weckström, Jan., Rosén, P., Ryves, D. B., Roberts, S. J., and
Schmidt, R.: A lacustrine GDGT-temperature calibration from the Scandinavian Arctic to
Antarctic: renewed potential for the application of GDGT-paleothermometry in lakes, *Geochim.*
Cosmochim. Acta, 75, 6225-6238, doi: 10.1016/j.gca.2011.07.042, 2011.

Peterse, F., van der Meer, J., Schouten, S., Weijers, J. W. H., Fierer, N., Jackson, R. B., Kim, J. M.,
and Sinninghe Damsté, J. S.: Revised calibration of the MBT-CBT paleotemperature proxy based
on branched tetraether membrane lipids in surface soils, *Geochim. Cosmochim. Acta*, 96,
215-229, doi:10.1016/j.gca.2012.08.011, 2012.

609 Peterse, F., Vonk, J. E., Holmes, R. M., Giosan, L., Zimov, N., and Eglinton, T. I.: Branched glycerol
 610 dialkyl glycerol tetraethers in Arctic lake sediments: sources and implications for
 611 paleothermometry at high latitudes, *J. Geophys. Res.-Biogeosci.*, 119, 1738-1754, doi:
 612 10.1002/2014jg002639, 2014.

613 Qian, S., Yang, H., Dong, C. H., Wang, Y. B., Wu, J., Pei, H. Y., Dang, X. Y., Lu, J. Y., Zhao, S. J., and
 614 Xie, S. C.: Rapid response of fossil tetraether lipids in lake sediments to seasonal environmental
 615 variables in a shallow lake in central China: Implications for the use of tetraether-based proxies,
 616 *Org. Geochem.*, 128, 108-121, doi:10.1016/j.orggeochem.2018.12.007, 2019.

617 Rao, Z. G., Jia, G. D., Li, Y. X., Chen, J. H., Xu, Q. H., and Chen, F. H.: Asynchronous evolution of
 618 the isotopic composition and amount of precipitation in north China during the Holocene
 619 revealed by a record of compound-specific carbon and hydrogen isotopes of long-chain
 620 *n*-alkanes from an alpine lake, *Earth Planet. Sci. Lett.*, 446, 68-76,
 621 doi:10.1016/j.epsl.2016.04.027, 2016.

622 Russell, J. M., Hopmans, E. C., Loomis, S. E., Liang, J., and Sinninghe Damsté, J. S.: Distributions of
 623 5- and 6-methyl branched glycerol dialkyl glycerol tetraethers (brGDGTs) in East African lake
 624 sediment: Effects of temperature, pH, and new lacustrine paleotemperature calibrations, *Org.*
 625 *Geochem.*, 117, 56-69, doi:10.1016/j.orggeochem.2017.12.003, 2018.

626 Schoon, P. L., de Kluijver, A., Middelburg, J. J., Downing, J. A., Sinninghe Damsté, J. S., and

Schouten, S.: Influence of lake water pH and alkalinity on the distribution of core and intact polar branched glycerol dialkyl glycerol tetraethers (GDGTs) in lakes, *Org. Geochem.*, 60, 72-82, doi:10.1016/j.orggeochem.2013.04.015, 2013.

Schouten, S., Huguet, C., Hopmans, E. C., Kienhuis, M. V. M., and Sinninghe Damsté, J. S.: Improved analytical methodology of the TEX86 paleothermometry by high performance liquid chromatography/atmospheric pressure chemical ionization-mass spectrometry, *Anal. Chem.*, 79, 2940-2944, doi:10.1021/ac062339v, 2007.

Schouten, S., Hopmans, E. C., and Sinninghe Damsté, J. S.: The organic geochemistry of glycerol dialkyl glycerol tetraether lipids: a review, *Org. Geochem.*, 54, 19-61, doi:10.1016/j.orggeochem.2012.09.006, 2013.

Shanahan, T. M., Huguen, K. A., and Van Mooy, B. A. S.: Temperature sensitivity of branched and isoprenoid GDGTs in Arctic lakes, *Org. Geochem.*, 64, 119-128, doi:10.1016/j.orggeochem.2013.09.010, 2013.

Shen, Z. W., Liu, J. B., Xie, C. L., Zhang, X. S., and Chen, F. H.: An environmental perturbation at AD 600 and subsequent human impacts recorded by multi-proxy records from the sediments of Lake Mayinghai, North China, *The Holocene*, 28, 1870-1880, doi:10.1177/0959683618798159, 2018.

Sinninghe Damsté, J. S., Hopmans, E. C., and Pancost, R. D.: Newly discovered non-isoprenoid

glycerol dialkyl glycerol tetraether lipids in sediments, *Chem. Commun.*, 23, 1683-1684,
doi:10.1039/b004517i, 2000.

Sinninghe Damsté, J. S., Ossebaar, J., Abbas, B., Schouten, S., and Verschuren, D.: Fluxes and
distribution of tetraether lipids in an equatorial African lake: Constraints on the application of the
TEX86 palaeothermometer and BIT index in lacustrine settings, *Geochim. Cosmochim. Acta*, 73,
4232–4249, doi:10.1016/j.gca.2009.04.022, 2009.

Sinninghe Damsté, J. S.: Spatial heterogeneity of sources of branched tetraethers in shelf systems: The
geochemistry of tetraethers in the Berau River delta (Kalimantan, Indonesia), *Geochim.
Cosmochim. Acta*, 186, 13-31, doi:10.1016/j.gca.2016.04.033, 2016.

Sun, Q., Chu, G. Q., Liu, M. M., Xie, M. M., Li, S. Q., Ling, Y., Wang, X. H., Shi, L. M., Jia, G. D.,
and Lü, H. Y.: Distributions and temperature dependence of branched glycerol dialkyl glycerol
tetraethers in recent lacustrine sediments from China and Nepal, *J. Geophys. Res.*, 116, G01008,
doi: 10.1029/2010jg001365, 2011.

Tian, L. P., Wang, M. Y., Zhang, X., Yang, X. Q., Zong, Y. Q., Jia, G. D., Zheng, Z., and Man, M. L.:
Synchronous change of temperature and moisture over the past 50 ka in subtropical southwest
China as indicated by biomarker records in a crater lake, *Quat. Sci. Rev.*, 212, 121-134, doi:
10.1016/j.quascirev.2019.04.003, 2019.

Tierney, J. E., and Russell, J. M.: Distributions of branched GDGTs in a tropical lake system:

implications for lacustrine application of the MBT/CBT paleoproxy, *Org. Geochem.*, 40,
1032-1036, doi:10.1016/j.orggeochem.2009.04.014, 2009.

Tierney, J. E., Russell, J. M., Eggermont, H., Hopmans, E. C., Verschuren, D., and Sinninghe Damsté,
J. S.: Environmental controls on branched tetraether lipid distributions in tropical East African
lake sediments, *Geochim. Cosmochim. Acta*, 74, 4902-4918, doi:10.1016/j.gca.2010.06.002,
2010.

Tierney, J. E., Schouten, S., Pitcher, A., Hopmans, E. C., and Sinninghe Damsté, J. S.: Core and intact
polar glycerol dialkyl glycerol tetraethers (GDGTs) in Sand Pond, Warwick, Rhode Island (USA):
insights into the origin of lacustrine GDGTs, *Geochim. Cosmochim. Acta*, 77, 561-581, doi:
10.1016/j.gca.2011.10.018, 2012.

Wang, H. Y., Liu, W. G., Zhang, C. L., Wang, Z., Wang, J. X., Liu, Z. H., and Dong, H. L.:
Distribution of glycerol dialkyl glycerol tetraethers in surface sediments of Lake Qinghai and
surrounding soil, *Org. Geochem.*, 47, 78-87, doi:10.1016/j.orggeochem.2012.03.008, 2012.

Wang, H. Y., Liu, W. G., Lu, H. X.: Appraisal of branched glycerol dialkyl glycerol tetraether-based
indices for North China, *Org. Geochem.*, 98, 118-130, doi:10.1016/j.orggeochem.2016.05.013,
2016.

Wang, M. Y., Zheng, Z., Zong, Y. Q., Tian, L. P.: Distributions of soil branched glycerol dialkyl
glycerol tetraethers from different climate regions of China, *Sci Rep.*, 9, 2761,

doi:10.1038/s41598-019-39147-9, 2019.

Weber, Y., De Jonge, C., Rijpstra, W. I. C., Hopmans, E. C., Stadnitskaia, A., Schubert, C. J.,
Lehmann, M. F., Sinninghe Damsté, J. S., and Niemann, H.: Identification and carbon isotope
composition of a novel branched GDGT isomer in lake sediments: evidence for lacustrine
branched GDGT production, *Geochim. Cosmochim. Acta*, 154, 118-129,
doi:10.1016/j.gca.2015.01.032, 2015.

Weber, Y., Sinninghe Damsté, J. S., Zopfi, J., De Jonge, C., Gilli, A., Schubert, C. J., Lepori, F.,
Lehmann, M. F., and Niemann, H.: Redox-dependent niche differentiation provides evidence for
multiple bacterial sources of glycerol tetraether lipids in lakes, *Proc. Natl. Acad. Sci. USA*, 115,
10926-10931, doi:10.1073/pnas.1805186115, 2018.

Weijers, J. W. H., Schouten, S., Spaargaren, O. C., and Sinninghe Damsté, J. S.: Occurrence and
distribution of tetraether membrane lipids in soils: Implications for the use of the TEX86 proxy
and the BIT index, *Org. Geochem.*, 37, 1680-1693, doi:10.1016/j.orggeochem.2006.07.018,
2006a.

Weijers, J. W. H., Schouten, S., Hopmans, E. C., Geenevasen, J. A. J., David, O. R. P., Coleman, J. M.,
Pancost, R. D., and Sinninghe Damsté, J. S.: Membrane lipids of mesophilic anaerobic bacteria
thriving in peats have typical archaeal traits, *Environ. Microbiol.*, 8, 648-657,
doi:10.1111/j.1462-2920.2005.00941.x, 2006b.

699 Weijers, J. W. H., Schouten, S., Van den Donker, J. C., Hopmans, E. C., and Sinninghe Damsté, J. S.:
700 Environmental controls on bacterial tetraether membrane lipid distribution in soils, *Geochim.*
701 *Cosmochim. Acta*, 71, 703-713, doi:10.1016/j.gca.2006.10.003, 2007a.

702 Weijers, J. W. H., Schefuß, N., Schouten, S., and Sinninghe Damsté, J. S.: Coupled thermal and
703 hydrological evolution of tropical Africa over the last deglaciation, *Science*, 315, 1701-1704,
704 doi:10.1126/science.1138131, 2007b.

705 Weijers, J. W. H., Wiesenberg, G. L. B., Bol, R., Hopmans, E. C., and Pancost, R. D.: Carbon isotopic
706 composition of branched tetraether membrane lipids in soils suggest a rapid turnover and a
707 heterotrophic life style of their source organism(s), *Biogeosciences*, 7, 2959-2973,
708 doi:10.5194/bgd-7-3691-2010, 2010.

709 Woltering, M., Werne, J. P., Kish, J. L., Hicks, R., Sinninghe Damsté, J. S., Schouten, S.: Vertical and
710 temporal variability in concentration and distribution of thaumarchaeotal tetraether lipids in Lake
711 Superior and the implications for the application of the TEX86 temperature proxy, *Geochim.*
712 *Cosmochim. Acta*, 87, 136-153, doi:10.1016/j.gca.2012.03.024, 2012.

713 Xiao, W. J., Wang, Y. H., Zhou, S. Z., Hu, L. M., Yang, H., Xu, Y. P.: Ubiquitous production of
714 branched glycerol dialkyl glycerol tetraethers (brGDGTs) in global marine environments: a new
715 source indicator for brGDGTs, *Biogeosciences*, 13, 5883–5894, doi:10.5194/bg-13-5883-2016,
716 2016.

717 Yang, H., Lü, X. X., Ding, W. H., Lei, Y. Y., Dang, X. Y., Xie, S. C.: The 6-methyl branched
718 tetraethers significantly affect the performance of the methylation index (MBT') in soils from an
719 altitudinal transect at Mount Shennongjia, Org. Geochem., 82, 42–53,
720 doi:10.1016/j.orggeochem.2015.02.003, 2015.

721 Zhang, J., Yu, Z. G., Jia, G. D.: Cyclisation degree of tetramethylated brGDGTs in marine
722 environments and its implication for source identification, Global Planet. Change, 184, 103043,
723 doi:10.1016/j.gloplacha.2019.103043, 2020.

724 Zhang, Z. H., Smittenberg, R. H., and Bradley, R. S.: GDGT distribution in a stratified lake and
725 implications for the application of TEX86 in paleoenvironmental reconstructions, Sci. Rep., 6,
726 34465, doi:10.1038/srep34465, 2016.

727 **Captions for Tables and Figures:**

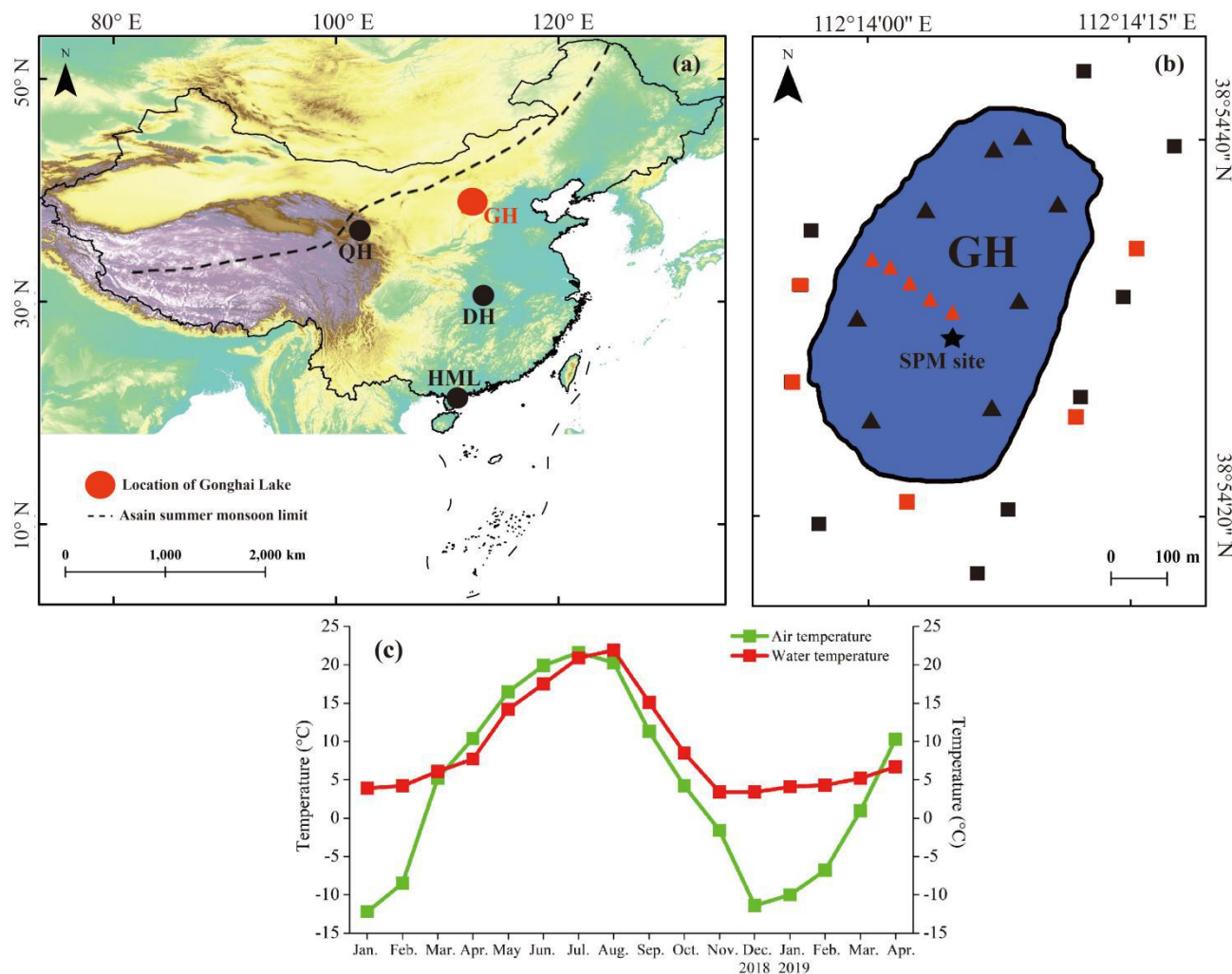


Fig. 1. (a) The Gonghai Lake (red circle), other referenced lakes (black circles) and modern Asian summer monsoon limit (dashed line; Chen et al., 2008). (b) SPM from water column (black star), surface soils (red squares) and surface sediments (red triangles) in Gonghai Lake in this study; black squares and triangles represents the sample sites published in Cao et al. (2017) (modified from Cao et al., 2017). (c) Measured local air temperature (AT) and lake water temperature (LWT) during 2018–2019 (this study).

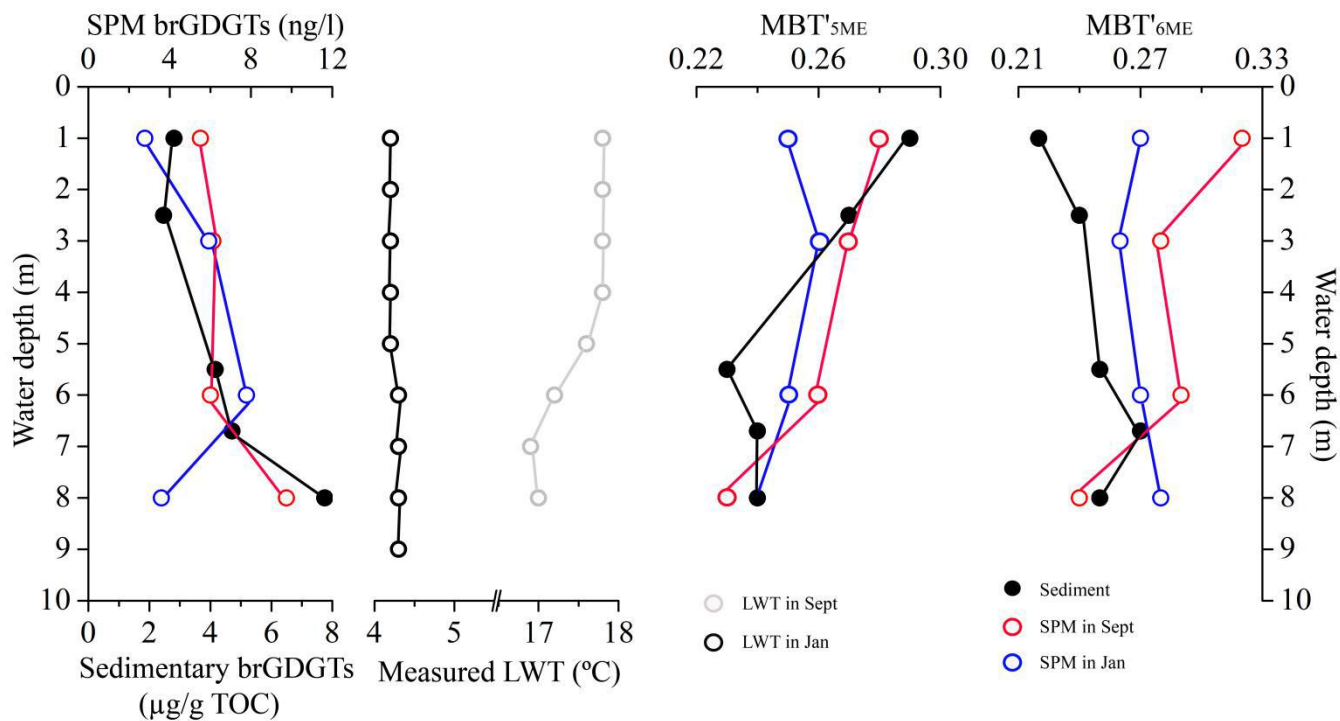


Fig. 2. Depth profiles of water temperature, brGDGT concentrations, MBT'_{5ME}, MBT'_{6ME} in water SPM from January and September and sediments in the Gonghai Lake.

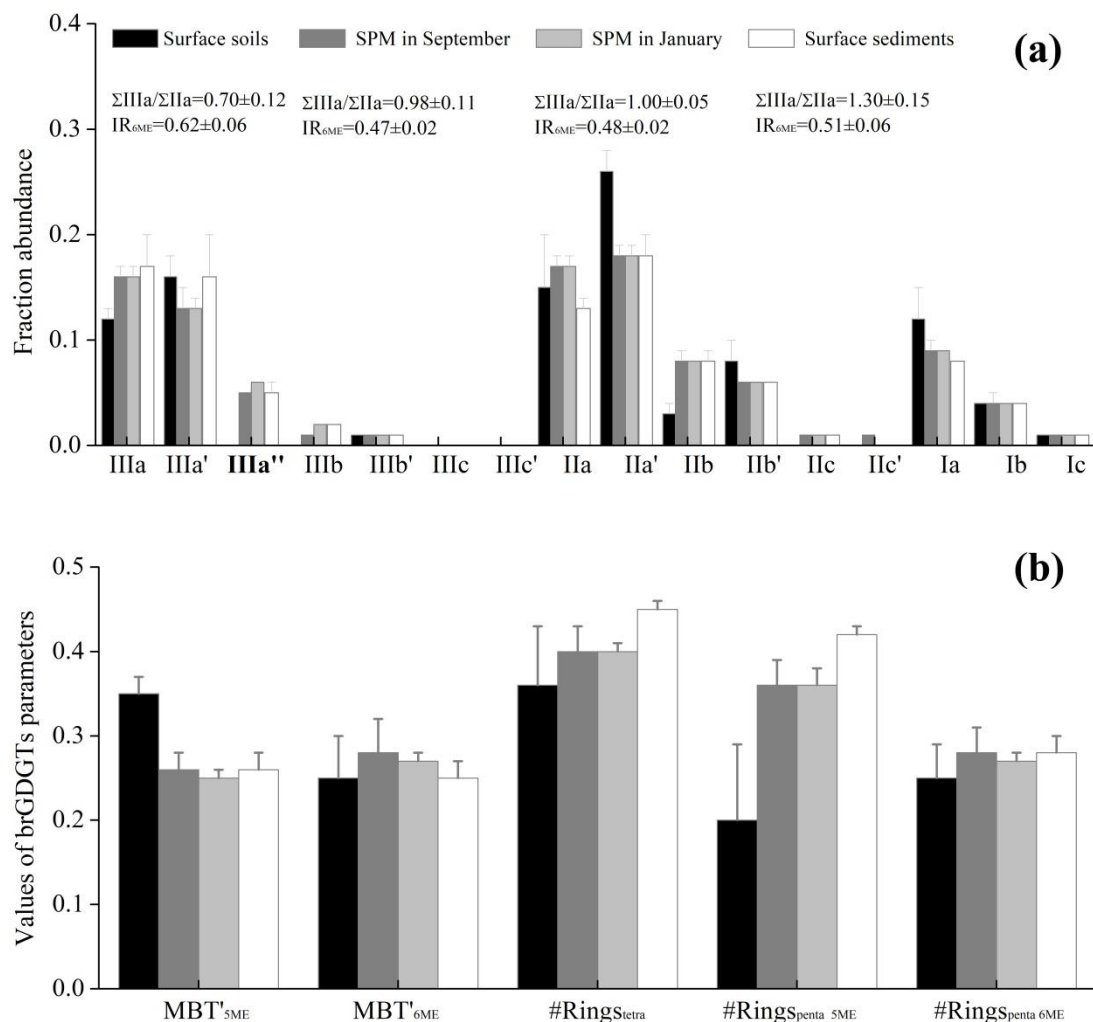


Fig. 3. BrGDGT distribution in surface soils, water column (SPM) and surface sediments of the Gonghai Lake. (a)

Fractional abundance of brGDGTs. (b) Degree of methylation and cyclisation of brGDGTs.

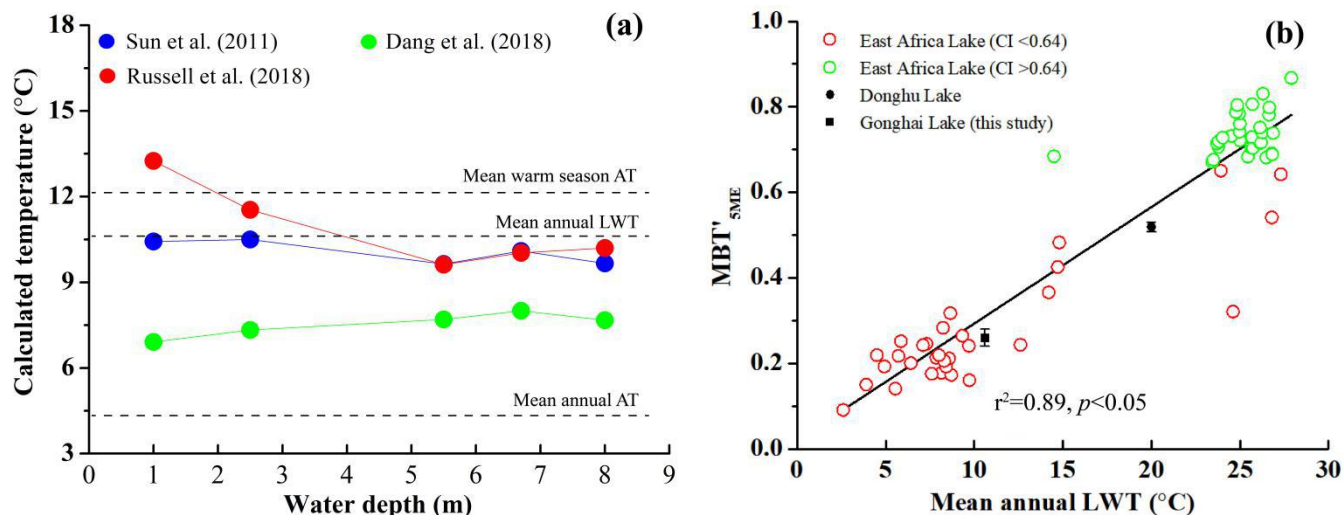


Fig. 4. (a) BrGDGT-derived temperatures for sediments using lake calibrations Eqs. (11), (15) and (16) from Sun et al. (2011), Dang et al. (2018) and Russell et al. (2018) respectively. (b) The correlation between MBT'_{5ME} of sedimentary brGDGTs and mean annual lake water temperature (LWT); CI index represents Community Index (De Jonge et al., 2019); the brGDGT data of East Africa Lake, Donghu Lake and Gonghai Lake were sourced from Russell et al. (2018), Qian et al. (2019) and this study.

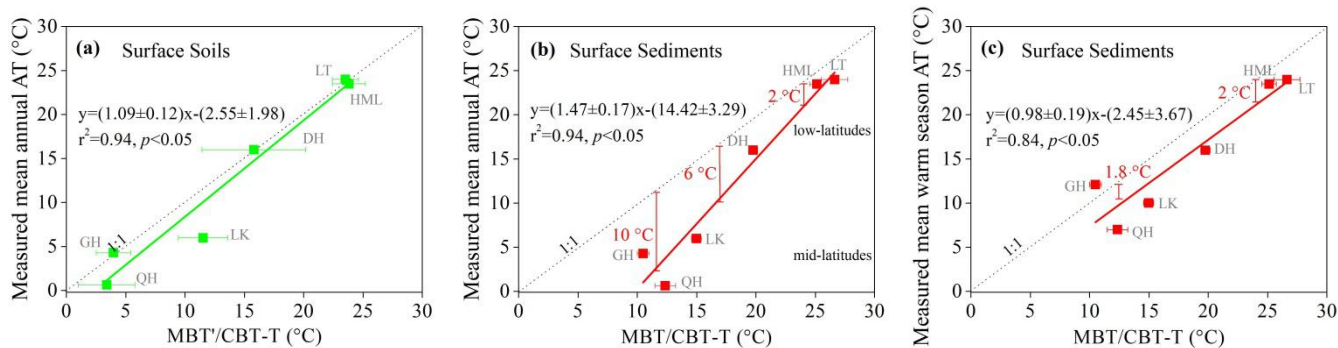


Fig. 5. Comparison of brGDGT-derived temperature and measured air temperature. (a) Measured mean annual AT and estimated temperatures of brGDGTs in surface soils based on soil calibration Eq. (9). (b) Measured mean annual AT and estimated temperatures of brGDGTs in surface sediments based on lake calibration Eq. (11). (c) Measured mean warm season AT and estimated temperatures of brGDGTs in surface sediments based on lake calibration Eq. (11). Data are from Gonghai Lake (GH; Cao et al., 2017), Lower King pond (LK; Loomis et al., 2014), Huguangyan maar (HML; Hu et al., 2015, 2016), Lake Donghu (DH; Qian et al., 2019), Qinghai Lake (QH; Wang et al., 2012) and Lake Towuli (LT; Tierney and Russell, 2009).

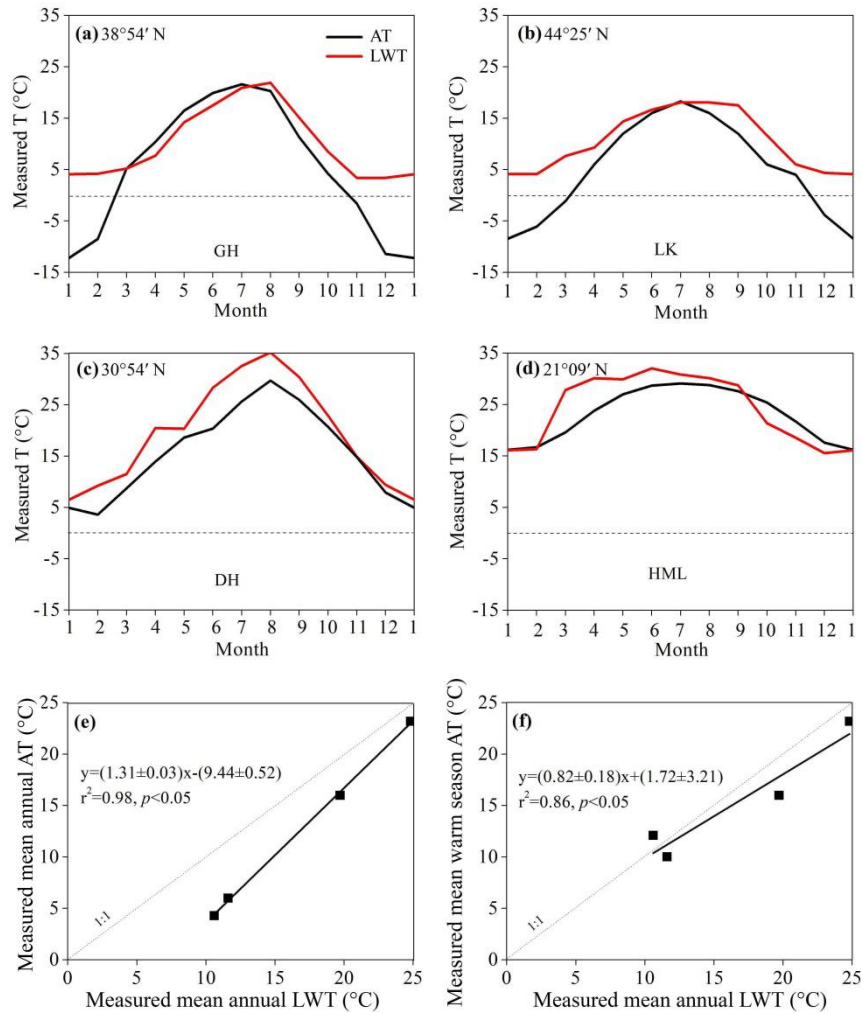


Fig. 6. Measured LWT and AT in (a) Gonghai Lake (GH; this study), (b) Lower King pond (LK; modified from Loomis et al., 2014), (c) Lake Donghu (DH; modified from Qian et al., 2019) and (d) Lake Huguangyan (HML; modified from Hu et al., 2016). (e) Correlation between mean annual AT and mean annual LWT. (f) Correlation between mean warm season AT and mean annual LWT. In the mid-latitude Gonghai Lake and Lower King pond, the surface LWT follows AT only when the AT is above freezing. In the low-latitude Lake Donghu and Lake Huguangyan, the surface LWT follows AT for the whole year.

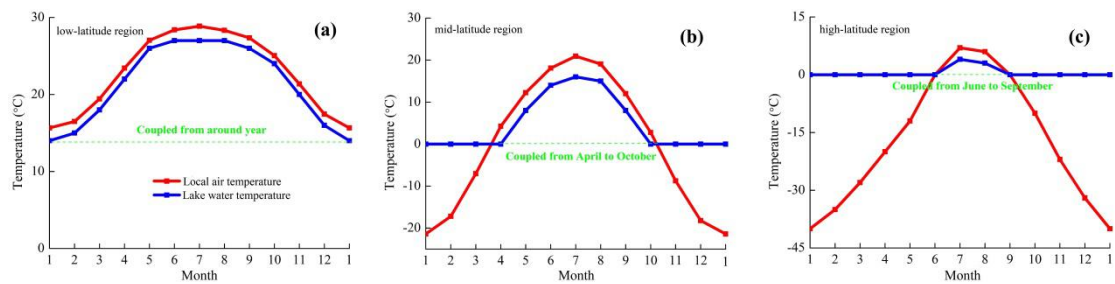


Fig. 7. A simple model showing the relationship between LWT and AT in different latitudes

Table 1 Concentration of brGDGTs, MBT'_{5ME}, MBT'_{6ME} and estimated temperatures in catchment surface soils, sediments and water column SPM in the Gonghai Lake.

Code of site	Longitude	Latitude	Vegetation type	Water depth (m)	IIIa"	Total brGDGTs			MAAT	MAAT	MAAT	MAAT	Growth				
	(E)	(N)			(ng/g dw)	MBT _{SME}	MBT _{6ME}	a (° C)						b (° C)	c (° C)	d (° C)	AT e
Surface soils in Gonghai catchment																	
S1	112° 14'19.039"	38° 54'37.343"	grass		0	74.82	0.31	0.21	1.20	-2.90							
S2	112° 14'18.460"	38° 54'28.750"	grass		0	23.50	0.36	0.20	2.58	-1.21							
S3	112° 14'24.140"	38° 54'23.098"	shrub		0	22.00	0.35	0.33	2.40	-4.22							
S4	112° 14'36.827"	38° 54'27.126"	shrub		0	32.65	0.36	0.26	2.64	-2.15							
S5	112° 14'40.502"	38° 54'38.174"	grass		0	16.06	0.36	0.24	2.82	-1.61							
Gonghai surface sediments																	
D1	112° 14'22.963"	38° 54'36.357"		1.00	1.46	42.03	0.29	0.22	0.70	-4.24	8.35	13.50	6.91				
D2	112° 14'24.004"	38° 54'35.903"		2.50	1.59	33.95	0.27	0.24	-0.13	-4.79	7.50	11.91	7.33				
D3	112° 14'25.109"	38° 54'35.294"		5.50	17.87	327.62	0.23	0.25	-1.19	-6.53	6.40	10.11	7.70				
D4	112° 14'27.301"	38° 54'34.499"		6.70	25.53	374.29	0.24	0.27	-0.93	-7.32	6.67	10.57	8.00				
D5	112° 14'28.453"	38° 54'33.980"		8.00	42.96	706.72	0.24	0.25	-0.95	-6.44	6.64	10.72	7.67				
Gonghai SPM in Sept																	
Water-1 m	112° 14'28.453"	38° 54'33.980"		1.00	0.29	5.71	0.28	0.32	0.24	-6.00	7.88	11.19	9.16				
Water-3 m	112° 14'28.453"	38° 54'33.980"		3.00	0.36	6.39	0.27	0.28	-0.05	-5.46	7.57	10.86	8.25				
Water-6 m	112° 14'28.453"	38° 54'33.980"		6.00	0.30	6.22	0.26	0.29	-0.35	-6.55	7.26	10.45	8.55				
Water-8 m	112° 14'28.453"	38° 54'33.980"		8.00	0.49	10.07	0.23	0.24	-1.40	-6.79	6.18	10.60	7.31				
Gonghai SPM in Jan																	
Water-1 m	112° 14'28.453"	38° 54'33.980"		1.00	0.16	2.88	0.25	0.27	-0.75	-6.32	6.85	10.40	7.95				
Water-3 m	112° 14'28.453"	38° 54'33.980"		3.00	0.36	6.09	0.26	0.26	-0.49	-5.57	7.12	11.02	7.77				
Water-6 m	112° 14'28.453"	38° 54'33.980"		6.00	0.49	8.05	0.25	0.27	-0.65	-6.24	6.95	10.57	7.99				
Water-8 m	112° 14'28.453"	38° 54'33.980"		8.00	0.22	3.71	0.24	0.28	-0.96	-6.89	6.63	10.20	8.24				

MAAT represents mean annual air temperature.

^a Calculated according to Eq. (9).
^b Calculated according to Eq. (10).
^c and ^d Calculated according to Eq. (16) and (17).
^e Calculated according to Eq. (15).

Table 2 Calibrations for brGDGT-derived temperature proxies used in this study.

Calibrations	Equation no. in the text	References
For soils		
MAAT=0.81-5.67*CBT+31.0*MBT ^a (<i>n</i> =176, <i>r</i> ² =0.59, RMSE=5.0 ° C)	(8)	Peterse et al. (2012)
MAAT=-8.57+31.45*MBT _{SME} (<i>n</i> =222, <i>r</i> ² =0.66, RMSE=4.8 ° C)	(9)	De Jonge et al. (2014)
MAAT ^a =27.63*Index 1-5.72 (<i>n</i> =148, <i>r</i> ² =0.75, RMSE=2.5 ° C)	(10)	Wang et al. (2016)
For sediments		
MAAT=6.803-7.062*CBT+37.09*MBT (<i>n</i> =139, <i>r</i> ² =0.62, RMSE=5.24 ° C)	(11)	Global, Sun et al. (2011)
MAAT=8.263-17.938*CBT+46.675*MBT (<i>n</i> =24, <i>r</i> ² =0.52, RMSE=5.1 ° C)	(12)	Regional, Sun et al. (2011)
MAAT ^b =50.47-74.18*f(IIIa)-31.60*f(IIa)-34.69*f(Ia) (<i>n</i> =46, <i>r</i> ² =0.94, RMSE=2.2 ° C)	(13)	Tierney et al. (2010)
MAAT=22.77-33.58*f(IIIa)-12.88*f(IIa)-418.53*f(IIc)+86.43*f(Ib) (<i>n</i> =111, <i>r</i> ² =0.94, RMSE=1.9 ° C)	(14)	Loomis et al. (2012)
Growth AT=21.39*MBT _{6ME} +2.27 (<i>n</i> =39, <i>r</i> ² =0.75, RMSE=1.78 ° C)	(15)	Dang et al. (2018)
MAAT=23.81-31.02*f(IIIa)-41.91*f(IIb)-51.59*f(IIb')-24.70*f(IIa)+68.80*f(Ib) (<i>n</i> =65, <i>r</i> ² =0.94, RMSE=2.14 ° C)	(16)	Russell et al. (2018)
MAAT=-1.21+32.42*MBT _{SME}	(17)	Russell et al. (2018)

775 AT represents air temperature.

MAAT represents mean annual air temperature.

^a Index=log[(Ia+Ib+Ic+IIa'+IIIa')/(Ic+IIa+IIc+IIIa+IIIa')].

^b Fractional abundance of brGDGTs is a fraction of only brGDGT Ia, IIa and IIIa.

Table 3 Comparison of measured air temperature, brGDGT-derived temperature from catchment soils and
brGDGT-derived temperature from sediments in different lake basins.

Name	Latitude	Longitude	Depth (m)	MAA	Mean warm season	Mean annual	Surface soils	Surface sediments					References
				T	AT	LWT		MAAT ^a	MAAT ^b	MAAT ^c	MAAT ^d	MAAT ^e	
				(° C)	(° C)	(° C)		(° C)	(° C)	(° C)	(° C)	(° C)	
Gonghai Lake	38° 54′	112° 14′	9	4.3	12.1	10.6	3.96±1.46	10.74±	10.86±				Cao et al. (2017)
	N	E						0.33	9.70±0.71	7.93±1.46			
Lake Towuti	2.5° S	121° E	200	24	24	n.d.	22.52± 2.61	26.62±	29.13±				Tierney and Russell. (2009)
								1.10	1.86	n.d.	n.d.		
Lake Huguanyan	21° 09′	110° 17′	20	23.2	23.2	24.8	23.80± 1.39	25.11±	28.12±	26.47±	26.07±		Hu et al. (2015, 2016)
	N	E						0.60	0.90	0.83	0.73		
Lake Donghu	30° 54′	114° 41′	6	16	16	20	15.79± 4.37	19.74±	22.82±	25.75±	20.61±		Qian et al. (2019)
	N	E						0.39	0.51	0.34	0.71		
Qinghai Lake	36° 54′	100° 01′	27	0.65	7	n.d.	3.38±2.40	12.34±		13.61±			Wang et al. (2012)
	N	E						0.87	9.92±1.14	1.49	8.80±1.11		
Lower King pond	44° 25′	72° 26′	8	6	11.3	11.6	11.50± 2.08	14.97±		18.75±	15.76±		Loomis et al. (2014)
	N	W						0.42	14.9±0.53	0.64	0.84		

AT represents air temperature and MAAT represents mean annual air temperature.

LWT represents lake water temperature.

^a Calculated after according to Eq. (8).

^b and ^c Calculated according to Eq. (11) and (12).

^d Calculated after according to Eq. (13).

^e Calculated after according to Eq. (14).